Electron (hole) paramagnetic resonance of spherical CdSe nanocrystals.

K. Gokhberg[1], A. Glozman[1], E. Lifshitz[1] , T. Maniv[1] , M.C. Schlamp[2] and P. Alivisatos[2]
[1] *Department of Chemistry and Solid State Institute, Technion–Israel Institute of Technology, Haifa 32000, Israel*
[2] *Department of Chemistry, University of California and Material Science Division, Lawrence Berkeley National Laboratory, Berkeley, Cal. 94720, USA*

A new mechanism of electron paramagnetic resonance in spherical zinc-blende semiconductor nanocrystals, based on the extended orbital motion of electrons in the entire nanocrystal, is presented. Quantum confinement plays a crucial role in making the resonance signal observable. The mechanism remains operative in nanocrystals with uniaxially distorted shape. A theoretical model based on the proposed mechanism is in good quantitative agreement with unusual ODMR spectra observed in nearly spherical CdSe nanocrystals.

Nearly two decades of research have explored the origin and potential applications of unusual opto-electronic properties of semiconducting nanocrystals. In particular, quantum size effects on nanometer length scale can lead to unique features in optical properties ([1], [2]) as compared to the corresponding properties of the bulk solids. Several reports have recently described the development of a new type of colloidal nanocrystals based on CdSe and CdS core coated with an epitaxial shell of a different semiconductor or by organic ligands ([3]- [5]).

The electronic properties of nanocrystals have been investigated extensively during the last decade (see e.g. [6], [7], [8] and references therein). However, there is still significant uncertainty regarding the orbital and spin dynamics of carriers in the presence of an external magnetic field, under the quantum confined conditions of the nanocrystals. In particular, a direct method for determining the carriers' effective masses in nanocrystals, similar to the cyclotron resonance technique used routinely in bulk semiconductors, is lacking. As will be shown in this paper, however, application of the Optically Detected Magnetic Resonance (ODMR) technique to nanocrystalline materials can provide the missing information by taking advantage of the quantum confinement imposed on the carriers dynamics.

Our recent ODMR study of CdSe and CdS nanocrystals has revealed unusually broad resonance bands which could not be accounted for in terms of the standard spin Hamiltonian model since such an interpretation would yield unreasonably large g-factors (i.e. in the range of $4-10$). In this paper we present a new mechanism of electron paramagnetic resonance in spherical semiconducting nanocrystals, based on the extended orbital motion of electrons in the entire nanocrystal, which can account for the observed resonance bands. In macroscopic crystals paramagnetic resonance of conduction electrons is strongly damped by the coupling to the lattice degrees of freedom (typical spin-lattice relaxation times T_1 are in the range of 10^{-10} to 10^{-8} sec. ([9])). The dramatic suppression of the relaxation rates in small nanocrystals (with $T_1 \sim 10^{-6} - 10^{-4}$ sec ([6])) due to the effect of quantum confinement can make these resonances easily observable.

Nanocrystals of CdSe, capped either with tri-octyphosphine-oxide (TOPO) or epitaxial layers of CdS with core diameter of about $30\mathring{A}$, were prepared according to the procedure described by Peng et al. ([10]). The photoluminescence (PL) and ODMR measurements were carried out by immersing the samples in a cryogenic dewar (at 1.4K) and exciting them with a continuous 457.9 nm Ar^+ laser. The sample was mounted on a special sample probe at the centre of a High-Q resonance cavity, coupled to a microwave (mw) source (10 GHz), and surrounded by a superconducting magnet (B). A detailed description of the experimental system is described in Ref.([6]). The ODMR spectra were obtained by measuring a change in luminescence intensity, due to the absorption of a modulated magnetic component of a microwave radiation. The latter was plotted (see Fig.1) versus the external magnetic field, B, yielding a magnetic resonance-like spectrum.

The PL spectra of CdSe (TOPO) and CdSe/CdS core-shell samples consist of an exciton band (centred at 2.15 eV), predominantly tunable with the size of the core, and an additional broad band at lower energies (centered at 1.70 eV). The exciton band in both samples did not show resonance phenomena and therefore, the ODMR spectra were selectively recorded around 1.7 eV. The ODMR spectrum of either CdSe(TOPO) or CdSe/CdS nanocrystals consisted of three broad resonance bands (Fig. 1a), ranging between 200-8500 Gauss. The spectrum of the CdSe/CdS core-shell structure showed additional overlapping narrow resonance bands (see inset in Fig. 1a) between 3000-5000 Gauss. The broad resonances were mainly pronounced upon an application of kHz mw power modulation, while the narrow resonances in CdSe/CdS were observed under a mw modulation of about 100Hz. This distinction suggests the existence of two types of magnetic resonance events, with different characteristic relaxation times. Furthermore, the appearance of the narrow resonances with g-factors close

to 2.000 (i.e. 1.988 and 1.845) in contrast to the broad ones, emphasizes the localized nature of the corresponding states within the forbidden band gap. The chemical identification of the corresponding trapping sites are discussed at length in a separate publication ([6]). They are considered as pure spin resonance transitions of trapped electrons and holes.

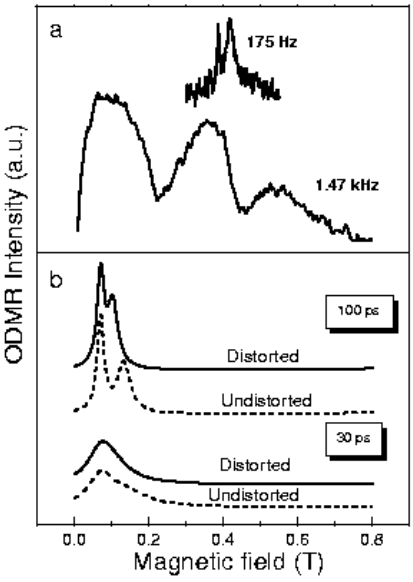

FIG. 1. (a) ODMR spectra of CdSe(TOPO) recorded at 1.47 kHz. The inset corresponds to the ODMR spectrum of CdSe(CdS) recorded at 175 Hz. (b) Calculated Lorentzian lines for the electronic 'p'-state multiplet in distorted and undistorted spherical nanocrystals. The corresponding lifetimes were taken to be 100 ps and 30 ps. Note the splitting for different values of F, which is weaker in the distorted nanocrystal.

The broad ODMR bands are reminiscent of cyclotron resonance data with cyclotron effective mass values in good agreement with the well known conduction and valence band effective masses of CdSe. It is evident, however, that well defined cyclotron orbits cannot exist within the nanocrystal's interior since the minimal cyclotron radius of an electron under the magnetic field used in such experiments is much larger than the size of a nanocrystal. Thus, the observed magnetic resonances cannot be associated with the field induced diamagnetic currents within the nanocrystals and should be assigned to a paramagnetic effect. They are most probably associated with transitions between initial extended electron (hole) states within the entire space of the nanocrystal and final localized hole (electron) states trapped in defect cites (shown schematically in Fig.2). The magnetic resonance events take place during the initial stages.

Focusing on the magnetic resonance processes we follow an approach exploited in Ref. ([12]), where the g-factor for acceptor levels in diamond-type semiconductors was calculated. The spherical symmetry of the electron (hole) wavefunctions at the Γ-point of the Brillouin zone simplifies the calculation considerably, leaving the crystal field and lattice effects to appear only through effective masses and g-factors. Within this approach the spherical symmetry is broken only at the nanocrystal surface, namely when some of the nanocrystal faces do not follow the elementary Wigner-Seitz polyhedron of the zinc-blende structure. Electron and hole are treated throughout the paper as independent particles. This is justified by the large electronic energy separation in a nanocrystal with respect to the electron-hole Coulomb interaction ([11]).

Near the Γ-point the conduction band of bulk CdSe is nearly parabolic, with isotropic effective mass tensor. Utilizing the effective mass and g-factor of an electron provided by the $\mathbf{k}\cdot\mathbf{p}$ theory, the relevant Hamiltonian is written in the form,

$$\hat{H} = \frac{1}{2m^*}\left(\mathbf{p} - \frac{e}{c}\mathbf{A}\right)^2 + g^*\mu_B \mathbf{S}\cdot\mathbf{B} + \hat{H}_{S.O.} \qquad (1)$$

where m^* is the conduction band effective mass at the Γ -point, g^* is the corresponding effective g-factor (i.e. corrected by the crystal field), and $\hat{H}_{S.O.}$ is the spin-orbit (SO) interaction.

Selecting the symmetric gauge form of the vector potential $\mathbf{A} = (0, 0, \frac{1}{2}Brsin\theta)$ to describe a constant and uniform magnetic field $\mathbf{B}$ aligned along the z-axis, with spherical polar coordinates (r, θ, ϕ) , Eq.(1) can be rewritten in the form: $\hat{H} = \mathbf{p}^2/2m^* + \hat{H}_{S.O.} + \beta(L_z + g_S S_z)B$, where the diamagnetic term, $(eBrsin\theta)^2/8m^*c^2$, is neglected. Here $\beta = \mu_B m_0/m^*$, $g_S = g^* m^*/m_0$, m_0 is the free electron mass, and L_z and S_z are, respectively, the projections of the orbital and spin angular momentum on the z-axis. In the presence of the spin-orbit interaction the eigenstates correspond to the total angular momentum $\mathbf{F} = \mathbf{L} + \mathbf{S}$, and the corrections to the electron energy due to the paramagnetic term are $\delta E_{el} = g_{F,el}\beta M_F B$, where $g_{F,el}$ is the electronic Lande factor, and M_F is the projection of $\mathbf{F}$ on the z-axis. Using a standard scheme, we find that $g_F = 1+(g_S-1)\alpha$, where $\alpha = \left[S(S+1) + F(F+1) - L(L+1)\right]/2F(F+1)$.

The corresponding calculation near the valence band edge is considerably more complicated due to the four-fold degeneracy of the band edge at the Γ-point. The relevant magnetic resonance transitions involve the Zeeman splitting of a hole near this energy. Since the energies involved are much smaller than the SO split-off energy Δ, the latter can be ignored ([12]). Thus, the motion of holes near the band edge in the presence of the magnetic field can be described by Luttinger Hamiltonian ([13]),

$$\hat{D} = \frac{1}{m_0}\left\{(\gamma_1 + \frac{5}{2}\gamma)\frac{k^2}{2} - \gamma(\mathbf{k}\cdot\mathbf{J})^2 + (\kappa - \frac{\gamma}{2})\frac{e}{c}\mathbf{J}\cdot\mathbf{B}\right\}, \qquad (2)$$

where γ, γ_1, and κ are Luttinger band parameters, $\mathbf{k} = \mathbf{p} - \frac{e}{c}\mathbf{A}$ and $\mathbf{J}$ is the set of 4×4 matrices of spin 3/2. In the absence of the magnetic field the $\mathbf{k}\cdot\mathbf{p}$ Hamiltonian at the Γ-point is invariant under rotations so that the total angular momentum $\mathbf{F} = \mathbf{L} + \mathbf{J}$ is conserved, while the resulting energy eigenvalues are independent of M_F . The perturbation theory with respect to the paramagnetic term yields for the Zeman splitting of a hole near the band edge $\delta E_h = g_{F,h}\mu_B M_F B$, where $g_{F,h}$ is the Lande factor of a hole.

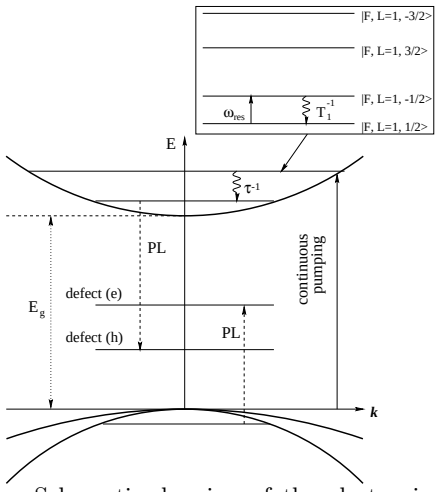

FIG. 2. Schematic drawing of the electronic spin-orbit energy levels invloved in the proposed ODMR mechanism. The spin-orbit 'p'-state manifold is shown in the inset. The relevant time scales are the Spin-lattice relaxation time $T_1 \sim 1 - 100$ μ s. , the non-radiative life-time $\tau_p \sim 1 - 200$ ps, and the magnetic resonance period $\omega_{res}^{-1} \sim 100$ ps.

The calculation of $g_{F,h}$ in the general case is complicated by the fact that in the corresponding unperturbed wavefunctions heavy and light hole components are mixed. A good approximation of $g_{F,h}$ can be obtained, however, in the limit $F \gg 1$, when the hole radial wavefunctions $R_{F,l}(r)$ ([14]) can be approximated by their asymptotic forms for which the motion of the heavy and light holes are completely decoupled. Consequently, the Zeeman energies of the holes can be written in a separable form, $\delta E^{hh} = [\gamma_1 - \frac{1}{2}\gamma]\mu_B M_F B, \delta E^{lh} = [\gamma_1 + \frac{1}{2}\gamma]\mu_B M_F B$, where 'lh' and 'hh' stand for light and heavy hole, respectively. The relevance of these simple limiting expressions to the present study will be discussed below.

The above analysis relied on the spherical symmetry of the nanocrystals under study. TEM pictures ([15]) however, showed that the nanocrystals are slightly elongated spheroids or ellipsoids. The effect of this symmetry breaking on the relevant electron and hole paramagnetic states, was estimated by assuming small deviations from the spherical shape and by exploiting the perturbation theory. A uniaxial shape distortion introduces an energy, $\hat{H}_{SD}$, which is typically much smaller than $\hat{H}_{SO}$, but much larger than the Zeeman spitting $\hat{H}_Z$ (see below). Thus, the perturbative procedure can be carried out in two stages, within the framework of the distorted wave Born approximation.

We consider the case of an electron near the bottom of the conduction band and use a model of a free particle enclosed in a nearly spherical cavity slightly distorted along some axis. The first order correction to energy due to this distortion is given by $\delta E^{SD}_{n,l,F,M_F} = \epsilon E^0_{n,l,F}\left[M_F^2/F(F+1) - 1/3\right]$, where $E^0_{n,l,F}$ is the corresponding unperturbed energy, $\epsilon = 2(a-b)/(a+b)$ is the deformation parameter, assumed to be small, a and b are the principal semiaxes of the ellipsoid. Note that in the latter formula the z-axis is selected along the symmetry axis of the nanocrystal.

Due to this uniaxial distortion the original $2F+1$ fold degenerate multiplet splits into a collection of Kramers' doublets, each of which having the same value of $|M_F|$. For the prolate nanocrystals the lowest lying doublet corresponds to $M_F = \pm 1/2$ and the highest one has $|M_F| = F$. In the oblate case the picture is reversed.

It is important to note that, due to the finite size of the electron wavefunctions (i.e. $R \sim 3 - 4nm$), the minimal value of the unperturbed energy $E^0_{n,l,F} \sim \hbar^2 R^{-2}/2m^*$ is typically much larger than the Zeeman energy $\sim \beta M_F B$; consequently, the distortion energy, $\delta E^{SD}_{n,l,F,M_F}$, is significantly larger than $\beta M_F B$.

An external static magnetic field $\mathbf{B}$, lifts the residual degeneracy of the Kramers' doublets. When the field is not aligned along the nanocrystal's symmetry axis, one should use the more general form $\hat{H}_Z = g_F\beta\mathbf{F}\cdot\mathbf{B}$. The corresponding Zeeman splitting energy of the doublets with $|M_F| = 1/2$ is not given by the familiar formula $\delta E_Z = g_F\mu_B B cos\theta_0 M_F$, where θ_0 is the angle between $\mathbf{B}$ and the symmetry axis of the ellipsoid, since $\hat{H}_Z$ mixes the zero-order functions of the doublet with $M_F = \pm 1/2$. A slightly more complicated expression, $\delta E_Z = \pm 1/2 g_F\mu_B B[cos^2\theta_0 + (F + 1/2)^2 sin^2\theta_0]^{1/2}$, is obtained in this case, which reduces however to the $\theta_0 = 0$ expression, δE_{el} , at $F = 1/2$ for any θ_0. This dependence of the Zeeman splitting energy on F and θ_0 requires a careful calaculation of the observable position of the magnetic resonance peak, which takes into account the transition matrix element $M_{-1/2\leftrightarrow 1/2}$. It is easy to show that $\left|M_{-1/2\leftrightarrow 1/2}\right| = A(F+\frac{1}{2})\left|\cos 2\theta_0\right|/2\left[\cos^2\theta_0 + (F+\frac{1}{2})^2\sin^2\theta_0\right]^{1/2}$, where A is constant, independent of θ_0 and F.

Application of the microwave magnetic field in a plane perpendicular to $\mathbf{B}$ causes transitions of significant intensity between different Zeeman split sublevels satisfying the selection rule $\Delta M_F = \pm 1$. Considering first only the nanocrystals with symmetry axes parallel to $\mathbf{B}$ (i.e. where $\theta_0 = 0$), it can be seen that among all the transitions satisfying the selection rule, only those originating from the $M_F = \pm 1/2$ doublet can be observed at magnetic field B in the experimentally accessible range. This is due, on the one hand, to the large distortion energy

$\delta E^{SD}_{n,l,F,M_F}$ and, on the other hand, to the the Kramers' degeneracy of the $M_F = \pm 1/2$ states in the distorted nanocrystals. Similar behavior is anticipated for the hole transitions, though the corresponding quantitative analysis of the shape distortion is quite involved ([7]).

The present ODMR spectra was monitored at the PL broad band, centered well below the bandgap energy. Thus it is assigned to transitions between excited electrons (holes) within spin-orbit states at the conduction (valence) band, recombining with holes (electrons) in defect levels, as shown schematically in Fig.2. As mentioned earlier, the spin-lattice relaxation time, T_1 , of the excited electrons and holes is in the range of 10^{-4}sec, while that of the trapped defect is of two orders of magnitude larger, thus suggesting that the spin flipping at the defect site can be considered stationary at the time scale of the spin flip within the spin-orbit manifold. Therefore, the spin splitting of the defect states was ignored in the model shown in Fig.2.

Let us first consider the ODMR band associated with the conduction electrons. For the excitation energy of the continuous Ar^+ laser used in the experiment only the ground ('s'-state; $S = 1/2, L = 0, F = 1/2$) and the first few excited F-states can be populated. Although the electrons pumped into an excited state relax quickly to the ground state via nonradiative channels, the observed ODMR band may be considered as arising mainly from $M_F = 1/2 \rightarrow -1/2$ transitions in such an excited state. Indeed, recent experiments have shown that in CdSe nanocrystals the life time, τ_p , of the first excited state ('p'-state; $S = 1/2, L = 1, F = 1/2$ and $S = 1/2, L = 1, F = 3/2$) is in the range of $1 - 200 \times 10^{-12}$sec. ([17], [18]). The corresponding decay rate, τ_p^{-1},which is much larger than the spin relaxation rate, T_1^{-1} , is of the same order of magnitude as the resonance microwave frequency, ω_{res} (see Fig.2). These imply that the spin excitation of electrons occupying the 'p'-state by the mw source can be completed before relaxing into the long-lived (luminescent) 's'-state, where their spin polarization is preserved for time much longer than the characteristic recombination time.

Assuming Lorentzian densities of F-states centered at δE_Z with frequency spread corresponding to τ_p^{-1} , and using the above expression for $M_{-1/2 \leftrightarrow 1/2}$, we find , after averaging over the angle θ_0 , the resonance lines shown in Fig.(1b) for typical values of τ_p. For the selected well known value of the electron effective mass $m^* = 0.13 m_0$, the calculated resonance position is in a very good agreement with the lower field resonance band observed in the experimental ODMR spectrum. In contrast , the calculated resonance peak due to spin excitations in the 's'-state appears at a field about 1.1T , well out of the field range shown in Fig.(1). It is interesting to note that the calculated integral intensity of this resonance is found to be much weaker than that of the 'p' state described above.

Evaluation of $g_{F,h}$ for the low-laying hole states has proved to be quite difficult. The corresponding resonance peak positions can be estimated, however, if we note that for $g_{F,el}$ in spherical nanocrystal all the levels of the multiplet with $L > 0$ (i.e. with the exception of $L = 0$, $F = 1/2$) cluster in the close vicinity of the multiplet's centre. The latter can be found by taking the mathematical limit $F \rightarrow \infty$ in the formula for δE_{el}. Assuming that the resonance lines of holes follow a similar pattern and using the above formulae for δE^{hh} and δE^{lh} together with the valence band parameters reported in ([8]) the centres of the respective multiplets are located at $B_{hh} = h\nu/(\gamma_1 - \frac{1}{2}\gamma)\mu_B$, $B_{lh} = h\nu/(\gamma_1 + \frac{1}{2}\gamma)\mu_B$, yielding $B_{hh} = 0.44$ Tesla and $B_{lh} = 0.33$ Tesla respectively. The value of B_{lh} is in close agreement with the maximum of the middle broad band shown in Fig.1. However, B_{hh} deviates slightly from the highest field band maximum, which is not surprising in view of the approximate nature of the present calculation.

In conclusion it was shown that the proposed mechanism of electron (hole) paramagnetic resonance in nearly spherical zinc-blende semiconductor nanocrystals accounts well for the unusual features observed in the ODMR spectra of $CdSe$ nanoparticles. The observability of the corresponding resonance bands is due to the small size (i.e. in the range of several nanometers) of the crystallites as well as to the Kramers' degeneracy of the energy levels, which cannot be lifted by any shape distortion of electrostatic origin.

The authors express their deepest gratitude to Prof. G. Kventsel, V. Zhuravlev and R. Guliamov for useful discussions. This research was supported by the Israel Science Foundation, grant no. 36599-12.5

[1] M. G. Bawendi et al., J. Chem. Phys., 96 (1992), 946
[2] A. Eychmuller et al., Phys. Chem., 95 (1), (1991), 79
[3] A.P. Alivisatos, J. Phys. Chem., 100 (1996) 13266
[4] A. Mews et al., Phys. Rev. B 53 (20) (1996), 13242
[5] A. Hasselbarth et al., J. Phys. Chem. 97 (1993), 5333 Chem. 93 (1989), 593
[6] E. Lifshitz et al., Feature Article, J. Phys. Chem. 104 (2000), 10449
[7] Al. L. Efros, A. V. Rodina, Physical Review B, 47(1993), 10005
[8] P. J. Norris, M. G. Bawendi, Phys. Rev. B 53 , (1996), 16338
[9] P.E.Pikus and A.N.Titov, in *Optical Orientation*, edited by F. Meier and B.P. Azkharchenya, North-Hollend, Amsterdam, 1984, pp.73-131.
[10] X. Peng et al., J. Am. Chem. Soc. 119 (1997), 7019.
[11] Al.L. Efros, A.L. Efros, Sov. Phys. Semicond. 16(7), 1982
[12] B.L. Gel'mont, M. I. D'yakonov, Sov. Phys. Semicond., Vol. 7 (1345), 1974
[13] J.M. Luttinger, Phys. Rev. 102(1030), 1956
[14] G.B.Grigoryan et. al., Sov. Phys. Solid State 32(6),1031,

(1990)
[15] A. V. Kadavanich et al., MRS Symp. Proc. Vol.452, (1997), 353
[16] M. W. Lee and H. D. Drew, Solid State Communications, 62, (1987), 825
[17] V. I. Klimov et al, Phys. Rev. B 60 , (1999), 13740
[18] P. Guyot-Sionnest et al, Phys. Rev. B 60 , (1999) R2181